Single Phase Power Sensing with Developed Voltage and Current Sensors

Vicky Mudeng, Himawan Wicaksono, Andreas T. Destanio, and Yusuf Nainggolan
Institut Teknologi Kalimantan

Keywords: Power, Voltage, Current, Full-wave rectifier, Differential amplifier

Abstract: A power sensor measures single-phase electrical power involving both voltage and current sensors. This sensors' pair utilizes a full-wave rectifier and differential amplifier as signal conditioning circuits for sensing voltage and current, respectively. Power can be obtained with multiplication between voltage and current. In this study, an alternating current is converted to direct current using a full-wave rectifier by calibrating a capacitor filter to understate ripple voltage. In addition, a differential amplifier yields output voltage interpreting line voltage and current in root mean square for voltage and current sensors, respectively. The work within this study develops voltage and current sensors to measure power on load from a grid. We employ a theoretical calculation to calculate ripple voltage, peak voltage, the mean voltage of the rectifier, as well as output voltage of the differential amplifier. Additionally, we simulate the voltage and current sensor circuits to verify the theoretical results by applying different alternating current power. The results indicate that the voltage and current sensors can be effective for measuring single-phase electrical power.

1 INTRODUCTION

The multiplication between voltage and current produces electrical power. Therefore, a pair of sensors for measuring electrical power possesses a voltage and current sensors. A universal sensor to measure voltage, current, or temperature was conducted. A voltage divider consists of a negative or positive temperature coefficient (NTC/PTC), shunt, or common resistor was used for switching to only one type of sensor (Bouabana, 2016). Besides, an application of optical fiber as a high voltage measurement has been recognized. An optical voltage transducer proposed many extending in linear performance, wider dynamic range, lighter weight, smaller size, and safety compared with regular inductive transformer (Ribeiro, 2013). In addition, the all-digital on-chip voltage sensor monitor voltage transient employing a relative reference model was demonstrated. Also, a voltage sensor could convert the measured voltage to binary codes (Chung, 2016). A new configuration of voltage sensors based on fiber optic consist of $Bi_{12}TiO_{20}$ crystal was reported. The voltage sensor simultaneously determined the voltage and temperature with operating at 633 and 976 nm of wavelengths (Filippov, 2000).

On the other hand, a review of current sensing techniques was presented. A fundamental principle for sensing currents, such as Ohm's law of resistance, Faraday's law of induction, magnetic field sensor, and Faraday effect. In this review, a shunt resistor was used considerably due to more simple and accurate in low current measurement (Ziegler, 2009). Moreover, a highly precise magnetic current sensor was developed to measure ± 0-300 A deploying anisotropic magnetoresistance (Zhenhong, 2015). Additionally, a current sensor could be designed using a hall sensor (Yan, 2019). Research regarding novel rectangular yokeless current transducer was investigated for 400 amperes as a range of measurements. Despite, there were disadvantages of the designed sensor, for instance, a necessity of digital to analog converter (DAC) card, digital processing for the output signal, and high power consumption for multi-sensor systems (Chirtsov, 2018). A sensitive and effective dual measurement based on Johnson noise thermometry was presented. This new approach used a single tunneling magnetoresistive sensor with a high sensitivity of 250 mV/V/mT for measuring the current and temperature. The combination of field-programmable gate array (FPGA) and analog to digital converter (ADC) was able to obtain the two measured parameters. The

Mudeng, V., Wicaksono, H., Destanio, A. and Nainggolan, Y.
Single Phase Power Sensing with Developed Voltage and Current Sensors.
DOI: 10.5220/0009443201630168
In *Proceedings of the 1st International Conference on Industrial Technology (ICONIT 2019)*, pages 163-168
ISBN: 978-989-758-434-3

range measurements were ± 10 A and −40 °C to 160 °C for current and temperature, respectively (Liu, 2018).

An understanding of measuring voltage and current is fundamental to monitor electrical power on load, particularly for single-phase alternating current (AC) power. To the best of our knowledge, some of the authors of this paper have, for the first time to investigate a single-phase power sensor with a full-wave rectifier using four diodes and differential amplifier as signal conditioning circuits.

2 METHODS

2.1 Full-wave Rectifier

The aim of a full-wave rectifier is to transform an AC voltage (V_{AC}) to a direct current voltage (V_{DC}). The characteristic of the output voltage is either positive or negative voltage in the root mean square (RMS). This circuit has four diodes. However, only two diodes are conducted for each cycle. The use of a full-wave rectifier circuit in this study is to represent a set of AC voltage and current on the load at the primary coil of the transformer to be DC voltage and current at the transformer secondary coil for measuring electrical power on load from a grid. A transformer with a full-wave rectifier circuit, as well as a load resistance (R_{load}) are shown in Figure 1.

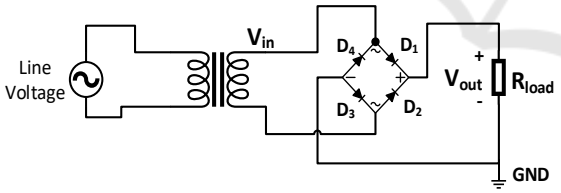

Figure 1: Circuit of full-wave rectifier system.

The output voltage (V_{out}) is yielded by the following equation.

$$V_{out}^{Peak} = V_{in}^{Peak} - (2.V_D) \quad (1)$$

$$V_{out}^{Peak} = V_{in}\sqrt{2} - (2.V_D) \quad (2)$$

$$V_{out} = \frac{V_{out}^{Peak}}{\sqrt{2}} \quad (3)$$

$$V_{out} = \frac{V_{in}\sqrt{2} - (2.V_D)}{\sqrt{2}}, \quad (4)$$

where, V_{in}^{Peak} and V_{out}^{Peak} are input and output peak voltage, respectively. V_D denotes diode voltage representing approximate 0.7 V due to it is a type of silicon semiconductor. As explained previously, the current for each cycle passes through two diodes, therefore 2. V_D = 1.4 V. In this form, V_{in} and V_{out} are in RMS with V_{in} is input voltage for the rectifier circuit.

The voltage waveforms of V_{in} and V_{out} for the full-wave rectifier are shown in Fig. 2. As can be seen, there is a drop voltage for V_{in}^{Peak} by discovering V_{out}^{Peak} due to the performance of two diodes in the circuit for each cycle. Farther, the negative part will be reversed to be positive voltage caused by diode two (D_2) and diode four (D_4). Thereunto, there is a time delay for the circuit to give the V_{out} due to the two diodes need times to conduction.

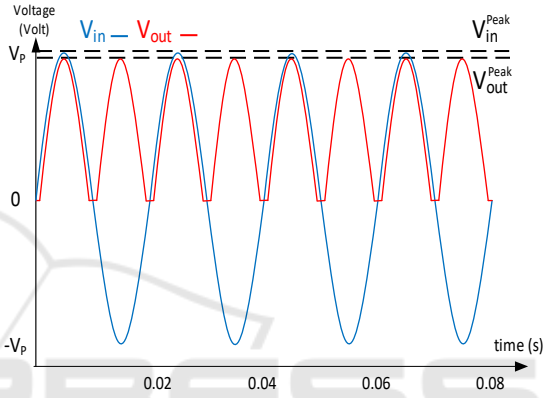

Figure 2: The waveform of V_{in} (blue line) and V_{out} (red line).

There are two procedures involving positive and negative sections for rectification. For the positive section, the current flows to diode one (D_1), then to R_{load}. Thereafter, the current will be streamed down to diode three (D_3) and return to the transformer. On the other hand, for the negative section, the current flows through D_2, then to R_{load}. Moreover, the current passes to D_4 and return to the transformer. The current constantly cross the R_{load}, thus obtains V_{out} under both positive or negative cycle. Therefore, even though in the negative cycle, the V_{out} will be a positive voltage. Figure 3 shows the current direction for each cycle.

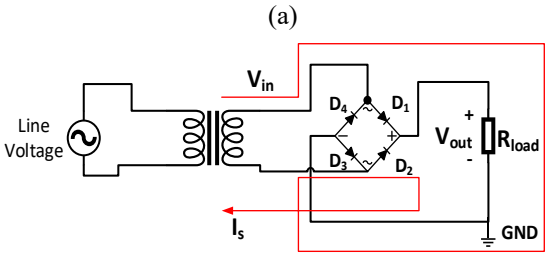

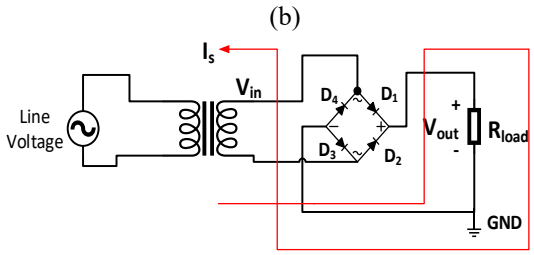

Figure 3: Current flow for (a) positive and (b) negative cycles of the full-wave rectifier circuit.

2.2 Capacitor Filter

The V_{out} from the rectifier is DC voltage with several ripples. In order to improve the rectification output, hence approaching the genuine DC voltage. Thus capacitor filter is utilized. The full-wave rectifier with a capacitor filter is shown in Figure 4.

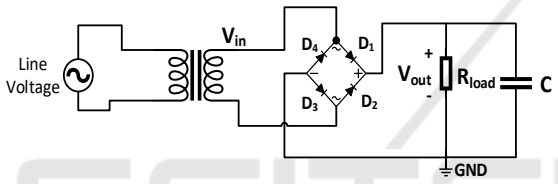

Figure 4: Full-wave rectifier circuit with a capacitor filter.

A ripple voltage (V_{ripple}) is a function of frequency and capacitance. With a certain frequency, as well as an appropriate capacitor, the V_{ripple} can be diminished and approach the DC voltage. Where the equation for V_{ripple} can be written as

$$V_{ripple} = \frac{I}{fC} \tag{5}$$

$$V_{ripple} = \frac{V_{out}^{Peak}}{R_{load} f C}, \tag{6}$$

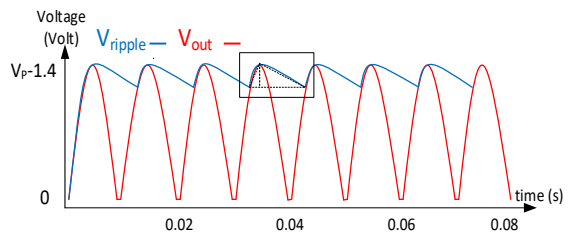

Figure 5: The waveform of V_{out} (red line) and V_{Ripple} (blue line).

R_{load} is load resistance, f denotes frequency on the grid ($f = 50\ Hz$), and C is capacitance value. Figure 5 depicts the V_{ripple} on the capacitor corresponding with V_{out}.

V_{DC} is yielded using Pythagoras' theorem, as can be seen inside the black square in Figure 5. Then, the illustration is the triangle inside the black square, as in Figure 6. With the triangle assumption, we can write the expression of V_{DC} as followed

$$x = \sqrt{(h_1 - h_2)^2 + (t_1 - t_2)^2}$$

$$Vrate_1 = h_1 - \frac{x}{2}$$

$$Vrate_2 = h_1 + \frac{x}{2}$$

$$V_{DC} = \frac{Vrate_1 + Vrate_2}{2}, \tag{7}$$

where x is hypotenuse voltage, h_1 and h_2 are peak and valley voltages of V_{ripple}, respectively. Additionally, $Vrate_1$ denotes the half voltage of x respect to h_1, while $Vrate_2$ is the half voltage of x respect to h_2 . Using Eq. (7), V_{DC} is discovered from the average value. It can be affirmed with the position of V_{DC} in the middle of the triangle (Priyanto, 2018), as shown in Figure 6.

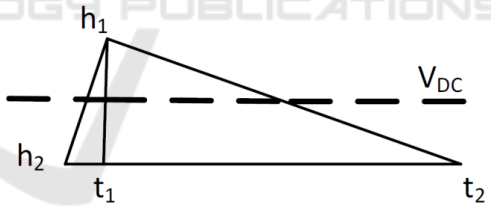

Figure 6: Triangle approach for calculating V_{DC}.

2.3 Differential Amplifier

In an ideal differential amplifier, it is using an analysis node at the inverting pin yields.

$$\frac{V_1 - V_-}{R_1} = \frac{V_- - V_{outamp}}{R_2}$$

$$\frac{V_1}{R_2} + \frac{V_{outamp}}{R_2} = \left(\frac{1}{R_1} + \frac{1}{R_2}\right) V_-$$

$$V_- = \frac{\frac{V_1}{R_1} + \frac{V_{outamp}}{R_2}}{\left(\frac{1}{R_1} + \frac{1}{R_2}\right)}, \tag{8}$$

due to negative feedback, therefore,

$$V_{-} = V_{+},$$

current summation on the non-inverting terminal obtains

$$\frac{V_2 - V_+}{R_1} = \frac{V_+ - V_{GND}}{R_2}, \quad (9)$$

substituting Eq. (8) to Eq. (9)

$$\frac{V_2 - \frac{\frac{V_1}{R_1} + \frac{V_{outamp}}{R_2}}{\left(\frac{1}{R_1} + \frac{1}{R_2}\right)}}{R_1} = \frac{\frac{\frac{V_1}{R_1} + \frac{V_{outamp}}{R_2}}{\left(\frac{1}{R_1} + \frac{1}{R_2}\right)}}{R_2}$$

$$V_2 R_2 - \frac{\frac{R_2 V_1}{R_1} + V_{outamp}}{\left(\frac{1}{R_1} + \frac{1}{R_2}\right)} = \frac{V_1 + \frac{R_1 V_{outamp}}{R_2}}{\left(\frac{1}{R_1} + \frac{1}{R_2}\right)}$$

$$V_{outamp} = \frac{(V_2 - V_1)\left(\frac{R_1 + R_2}{R_1}\right)}{\frac{R_1 + R_2}{R_2}}$$

$$V_{outamp} = \frac{R_2}{R_1}(V_2 - V_1), \quad (10)$$

R_1 is the input resistor corresponding to V_1 and V_2, whilst R_2 is the negative feedback resistor corresponding to inverting voltage (V_-). Also, R_2 denotes resistor of a voltage divider for input to non-inverting pin, and V_+ are non-inverting voltage. The output of the amplifier is V_{outamp} in this term. The circuit of the differential amplifier is shown in Figure 7.

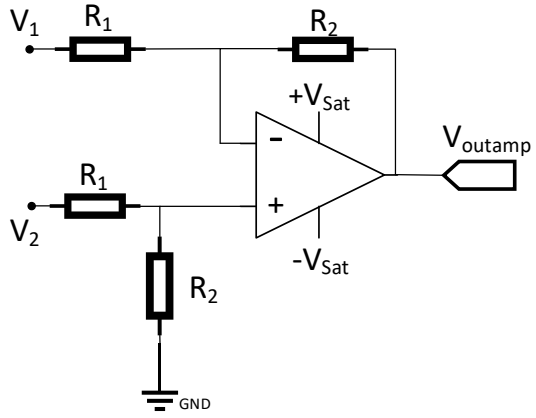

Figure 7: Differential amplifier circuit.

3 RESULTS

We developed a single-phase electrical power sensor composed of a voltage and current sensors. To measure a voltage, we need to put the metering on a source in parallel. Therewith, the metering to measure current is installed serially with the load. In this study, we had two sensing systems and combined them for measuring power. The full system of power sensor is shown in Figure 8.

In this system, we calculated the results based on theoretical knowledge and compared to the simulation results. Next, the results of the voltage sensor would be multiplied by the results of the current sensor with a microcontroller (μC). However, we did not discuss more regarding μC processing. This study emphasized in voltage sensor and current sensor represented by the system inside blue and red lines, as shown in Figure 8.

Furthermore, we established a voltage sensor with the specified line voltage, as in Table 1 column 1. Then, the next process was to determine the data as in Table 1 column 2-12. We performed one line voltage of $220V_{RMS}$ for the current sensor and added a set of the resistor on the primary coil of the transformer to obtain I_{Pcurr}, as in Table 2. Afterward, we could yield as in Table 2 column 5-14.

SW1, SW2, SW3, SW4 were the switches. If the SW1 and SW3 were opened, we obtained V_{out}^{Peak} volt and V_{out}^{Peak} current, respectively. On the other hand, if the SW1 and SW3 were closed, we obtained V_{DCvolt} and V_{DCcurr} using Eq. (7), simultaneously with $V_{ripplevolt}$ and $V_{ripplecurr}$. $V_{outampvolt}$ and $V_{outampcurr}$ could be yielded with closed all switches. The schematic of an electrical power sensor is shown in Figure 9. With Eq. (10), resistor values for the voltage sensor were $1k\Omega$ and 518Ω. Besides, $2.5k\Omega$ and 390Ω were for the current sensor. Further, we used capacitors of $400\ \mu F$ and $1\ nF$ as a capacitor filter for each sensor.

Moreover, we calculated relative error and its average (Priyanto, 2018) with the following equation.

$$Error(\%) = \left|\frac{Cal - Sim}{Cal}\right| . 100\%, \quad (11)$$

Where Cal denotes the calculated result, and Sim is a simulated result. As can be seen in Tables 1 and 2, the increase of average errors occurs in $V_{ripplevolt}$ and $V_{ripplecurr}$ for the measuring. But, these errors.

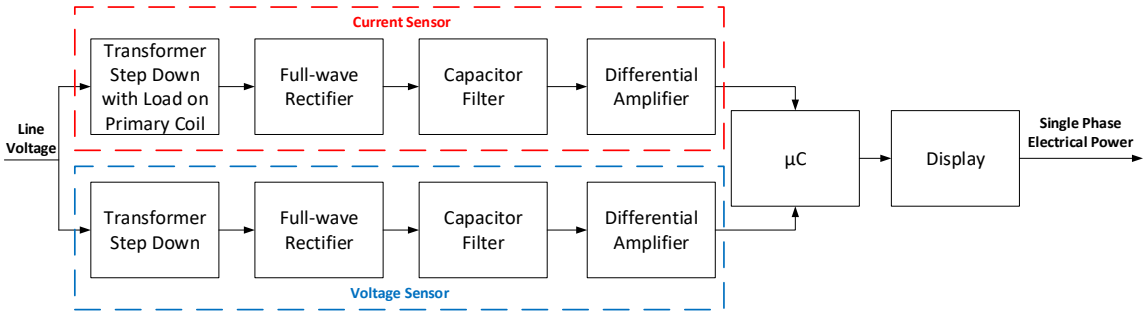

Figure 8: Full system of single-phase electrical power sensing.

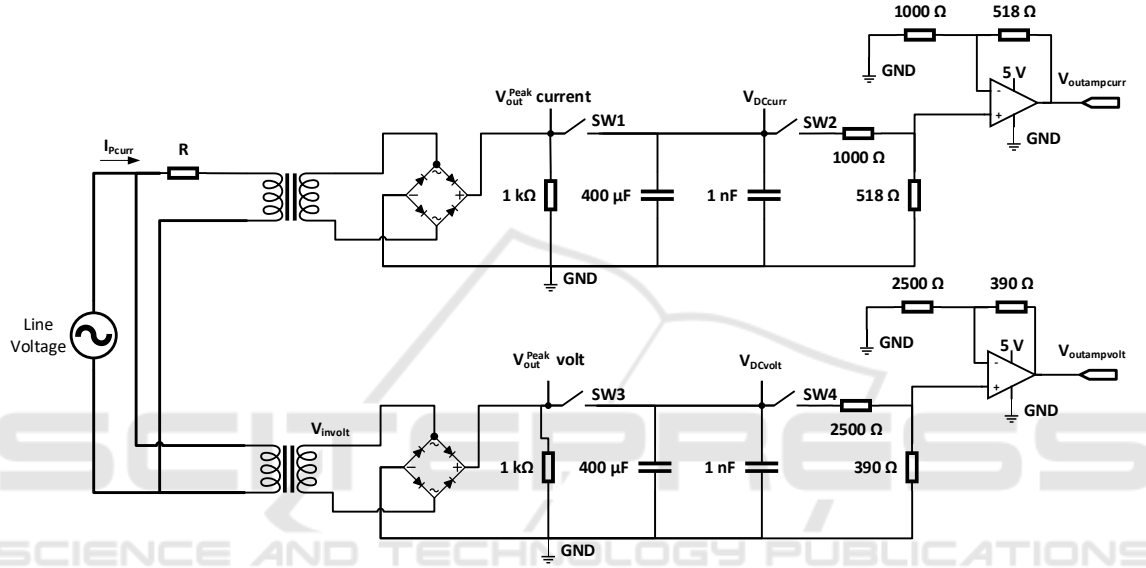

Figure 9: Schematic of a single-phase electrical power sensor.

Table 1: Results of the voltage sensor.

$V_{ripplevolt}$ (Volt)			V_{DCvolt} (Volt)			$V_{outampvolt}$ (Volt)		
Cal	Sim	Error (%)	Cal	Sim	Error (%)	Cal	Sim	Error (%)
0.0505	0.0560	10.9022	1.4028	1.4004	0.1680	0.2188	0.2191	0.1328
0.1505	0.1650	9.6384	4.1808	4.1740	0.1618	0.6522	0.6530	0.1246
0.3505	0.3820	8.9890	9.7368	9.7220	0.1517	1.5189	1.5208	0.1222
0.5505	0.5970	8.4481	15.2928	15.2720	0.1359	2.3857	2.3886	0.1216
1.1505	1.1810	2.6517	31.9608	31.9500	0.0337	4.9800	4.9919	0.2394
		8.1259			0.1302			0.1481

Table 2: Results of the current sensor.

R (Ohm)	I_{Pcurr}		V_{out}^{Peak} current (Volt)	$V_{ripplecurr}$ (Volt)			V_{DCcurr} (Volt)			$V_{outampcurr}$ (Volt)			
	Cal	Sim	Error (%)		Cal	Sim	Error (%)	Cal	Sim	Error (%)	Cal	Sim	Error (%)
2000	0.1100	0.1095	0.4545	5.1888	0.1835	0.1156	36.9974	5.0971	5.1172	0.3941	1.8672	1.8603	0.3713
1000	0.2200	0.2170	1.3636	7.7840	0.2752	0.2656	3.4931	7.6464	7.7010	0.7097	2.8011	2.7919	0.3295
500	0.4400	0.4224	4.0000	10.3776	0.3670	0.3652	0.4878	10.1941	10.2324	0.3743	3.7345	3.7309	0.0968
250	0.8800	0.7587	13.7841	12.4544	0.4404	0.4397	0.1535	12.2342	12.3129	0.6391	4.4818	4.4777	0.0917
125	1.7600	1.2103	31.2330	13.8368	0.4893	0.4866	0.5536	13.5922	13.6011	0.0655	4.9800	4.9823	0.0463
Average Error (%)			10.1670				8.3371			0.4365			0.1871

It did not affect the results of $V_{outampvolt}$ and $V_{outampcurr}$ due to V_{DCvolt} and V_{DCcurr} calculated by a triangle approach. With these results, we proved that the designed sensor is suitable for measuring electrical power.

4 CONCLUSIONS

We designed a single-phase electrical power sensor with both voltage and current sensors. Moreover, we compared between calculated and simulated results for each node in the designed sensor circuit. The results of voltage and current sensors would be multiplied; thus, we obtained the power. A comparison between calculated and simulated results indicated that the proposed power sensing sensor is potent to monitor electrical power on the grid.

ACKNOWLEDGMENT

This research was financially supported by the Ministry of Research, Technology, and Higher Education of the Republic of Indonesia through grant 007/SP2H/LT/DRPM/2019.

REFERENCES

Bouabana, Abdoulkarim, Erol Sanal, Constantinos Sourkounis, 2016. Development of A Low Cost Universal Sensor for An Accurate Measurement of Current, Voltage and Temperature. In 5th International Conference on Renewable Energy Research and Applications. IEEE.

Chirtsov, Andrey, Pavel Ripka, Jan Vyhnánek, 2018. Rectangular Array Current Transducer with Integrated Microfluxgate Sensors. In 2018 IEEE Sensors. IEEE.

Chung, Ching-. C, Mei-I. Sun, 2016. An All-Digital Voltage Sensor for Static Voltage Drop Measurements. IEEE Instrumentation and Measurement Society prior to the acceptance and publication.

Filippov, Valery N., Andrey N. Starodumov, Vladimir P. Minkovich, Francisco G. P. Lecona, 2000. Fiber Sensor for Simultaneous Measurement of Voltage and Temperature. IEEE Photonics Technology Letters, Vol. 12, No. 11.

Liu, Xu Y-., Philip W. T. Pong, Chun H-. Liu, 2018. Dual Measurement of Current and Temperature Using A Single Tunneling Magnetoresistive Sensor. In 2018 IEEE Sensors. IEEE.

Priyanto, Yun T. K., Vicky Mudeng, Andhika Giyantara, Ali Fahdian, Bima W. A. Achmadi, 2018. A Comprehensive Study of Alternating Current Voltage Sensor Using Rectifier and Operational Amplifier. In 2nd Borneo International Conference on Applied Mathematics and Engineering. IEEE.

Ribeiro, Bessie d. A., Marcelo M. Werneck, José L. d. S.-N., 2013. Novel Optimization Algorithm to Demodulate a PZT-FBG Sensor in AC High Voltage Measurements. IEEE Sensors Journal, Vol. 13, No. 4.

Yan, Hao, Yong X-. Xu, Wei D-. Zhao, He Zhang, Chris Gerada, 2019. DC Drift Error Mitigation Method for Three-Phase Current Reconstruction with Single Hall Current Sensor. IEEE Transactions on Magnetics, Vol. 55, No. 2.

Zhenhong, Zhang, Okabe Syuji, Akiyama Osamu, Konno Hideto, 2015. Development of the Highly Precise Magnetic Current Sensor Module of +/−300 A Utilizing AMR Element with Bias-Magnet. IEEE Transactions on Magnetics, Vol. 51, No. 1.

Ziegler, Silvio, Robert C. Woodward, Herbert H.-C. Iu, Lawrence J. Borle, 2009. Current Sensing Techniques: A Review. IEEE Sensors Journal, Vol. 9, No. 4.